Growth and Self-jumping of single condensed droplet on nanostructured surfaces: a molecular dynamics simulation

Jin Huan Pu[a], Si Kun Wang[a], Jie Sun[b*], Wen Wang[a] and Hua Sheng Wang[a*]

[a]*School of Engineering and Materials Science, Queen Mary University of London, London E1 4NS, UK*

[b]*School of Chemical Engineering and Technology, Xi'an Jiaotong University, Xi'an 710049, China*

[*]Authors to whom correspondence should be addressed. Electronic mails: sunjie@xjtu.edu.cn (JS); h.s.wang@qmul.ac.uk (HSW).

ABSTARCT: Our molecular dynamics simulation demonstrates that the condensed nanodroplets can achieve self-jumping off the nanostructured surface driven by the Laplace pressure difference, which has not yet been experimentally observed. The growth and self-jumping dynamics of nanodroplets condensed on the superhydrophobic nanostructured surface with local hydrophilic pinning site are systematically investigated. We reveal that a curvature difference between the droplet top and bottom is generated due to the confinement of the groove walls, which leads to a Laplace pressure difference. It increases with growing droplet and the droplet detaches from the groove valley and finally jumps off when it reaches the threshold against the pinning force from the hydrophilic pinning site. We find that the characteristics of the hydrophilic pinning site shows competitive effects on the whole process, which can be generally divided into incubation and burst stages. Increasing the surface wettability and size of the pinning site promotes the droplet growth but blocks the droplet self-jumping in the meantime due to the increased pinning force. We also find that the droplet-jumping highly depends on the confined portion of the droplet after detaching from the pinning site and its decrease will diminish the excessive surface energy stored in the droplet, which makes the converted kinetic energy insufficient to support the jump-off. The present work

sheds light on the fundamental understandings of passive method for condensate removal, self-cleaning, thermal management, etc.

Keywords: Individual droplet self-jumping; nanostructured surface; condensation; surface energy; molecular dynamics method.

1. Introduction

Surface condensation broadly exits in nature and industry [1][2] and is generally categorized into two modes: dropwise condensation (DWC) and filmwise condensation (FWC). Since DWC was discovered many decades ago, it has been given significant interest as its heat transfer coefficient is between 5 and 7 times that found with FWC [3]. DWC cycle starts from the nucleation of droplets, followed by their growth by either direct condensation or coalescence, and finally periodic departure from the surface. In this cycle, droplet departure from the surface has drawn much attention because it is vital to avoid surface flooding and to maintain efficient DWC [4]-[6]. In most condensing surfaces, droplet departure is commonly driven by gravitational force, which needs to overcome the contact line pinning force. Many efforts are paid to reduce the contact line pinning force and accelerate droplet departure, wherein lubricant-infused surfaces (LISs) have shown competitive advantages for both high- and low-surface-tension liquids [7]. Anand et al. [8] experimentally observed the remarkable mobility and the resultant sweeping effect of condensed drops on LISs and the moving speed of condensed droplets with size of 100 μm are several orders of magnitude higher than those on identically structured superhydrophobic surfaces. Smith et al. [9] showed that droplets on LISs have up to three different three-phase contact lines, which results in 12 different thermodynamic states. Guo et al. [10] revealed that the surface dynamic wettability of droplets on LISs during condensation process is dissimilar to their static wettability and the consistency between them is identified in their work. However, the performance of those surfaces highly depends on the existence of the lubricant but currently its depletion is inevitable, which will eventually cause LISs to lose their advantage.

Additionally, coalescence-induced droplet jumping is regarded as one of the efficient passive methods for achieving droplet departure, and lots of investigations have been carried out on its mechanistic understanding and application [11]-[20]. Boreyko et al. [11] first discovered the

spontaneous droplet removal resulting from the coalescence-induced droplet jumping and reported a surprising jumping velocity at a speed as high as 1 m/s. Miljkovic et al. [12] experimentally demonstrated highly efficient jumping-droplet condensation heat transfer on silanized copper oxide surfaces with a 25% higher overall heat flux and 30% heat transfer coefficient compared with conventional DWC on cooper surfaces at low supersaturations. Liang et al. [14] first demonstrated that the coalescence-induced jumping can also happen for nanoscale droplets although there is large internal viscous dissipation using molecular dynamics method. Yan et al. [17] developed a visualization technique to systematically study the effects of droplet size, surface structure, pinning, and liquid property on coalescence-induced droplet jumping. Shi et al. [20] first used lattice Boltzmann method to study the whole process of jumping-droplet condensation from nucleation to departure and even took the large amount of noncondensable gas into account. They found that the diameter and maximum jumping height of coalesced droplet decrease with the increase of noncondensable gas fraction. However, limited by coalescence hydrodynamics, the energy conversion efficiency (η) for the coalescence-induced droplet jumping process was experimentally and numerically reported to be less than 6%, corresponding to a dimensionless jumping velocity of 0.2-0.3 [21][22]. Meanwhile, previous studies show that the jumping velocity (v_j) of a coalescing droplet decreases with the droplet size increasing ($v_j \sim R_j^{-0.5}$) [11], which leads to larger droplets jumping, induced by coalescence, difficult. Additionally, this jumping process needs at least two droplets but for size-mismatched droplets, the jumping of coalescing droplet may fail due to the marginal kinetic energy [17].

In recent years, with the fast development of surface-nanomachining and surface-coating technologies, surface-structured-induced Laplace pressure difference stored within the droplet has been shown to trigger droplet departure or dewetting transition efficiently [23]-[28]. Lv et al. [23] reported an in situ spontaneous dewetting transition of condensed droplets on rigid

superhydrophobic pillared surfaces with two-tier roughness driven by the Laplace pressure difference. They also developed a theoretical expression to predict the Laplace pressure of the droplet and a model to characterize the critical size of the droplet when transition happens. Aili et al. [24] manufactured superhydrophobic nanostructured microporous surfaces to manipulate the droplet growth and jumping. They observed forced self-jumping of stretched droplets in pores and revealed that the excess surface free energy stored in the stretched droplet surface benefits this jumping. Sharma et al. [25] shows that the condensed droplets can spontaneously eject from even irregular, re-entrant, and random macrotextures driven by the Laplace pressure difference. Recently, Yan et al. [28] demonstrated that the jumping of a single-droplet driven by the Laplace-pressure contrast within the droplet is a much efficient passive method for droplet departure and it can achieve an ultra-high η up to 50-60%, with a dimensionless jumping velocity of 0.95.

However, due to the limitation of the observation technique and the difficulty of fully eliminating coalescence interference, most of previous experimental studies carried out the investigation about the characterization of the self-jumping of individual droplet without condensation and just artificially dispensed the droplet. Additionally, with the observation of the self-jumping of single-microdroplet driven by the Laplace pressure, it has been raised that if nanodroplet can also achieve self-jumping driven by the Laplace pressure difference stored within the droplet as viscous forces during droplet bursting becomes more significant in the nanoscale [28]. Molecular dynamics (MD) method has been widely used to investigate the surface condensation in nanoscale and provides an effective avenue to overcome the experimental limitation [29]-[33]. Therefore, in our work, we employed MD method to demonstrate the effectiveness of Laplace pressure driven single-nanodroplet jumping and clearly characterize the growth and self-jumping of single condensed droplet on super-hydrophobic nanostructured surface with local hydrophilic pinning site. Additionally, the effect

of the feature of the pinning site is preliminary discussed here. Our work enriches the understanding of the droplets self-jumping driven by the Laplace pressure and sheds light on the achievement of passive method for condensate removal, self-cleaning, thermal management and so on.

2. Computational methods

In this work, the growth and self-jumping of single condensed droplet on nanostructured surfaces were investigated using MD method. All the simulations are carried out using LAMMPS (large-scale/molecular massively parallel simulator) software package [34]. The simulation model consists of a superhydrophobic nano-groove with a hydrophilic pinning site and argon-like fluid, as shown in Fig. 1. The overall size of the simulation box measures $l_x \times l_y \times l_z = 80a \times 94a \times 142a$, where a is lattice constant with $a = 0.392$ nm. In the x and y directions, periodic boundary conditions are employed, while in the z direction, the fixed boundary condition is used, and the reflection boundary condition is also applied at the uppermost end. The nanostructured surface is constructed by Pt-like atoms arranged in a face-centered cubic (FCC) lattice with a lattice constant of 0.392 nm. To save the computational cost, the solid surface only consists of three layers of Pt-like atoms and one extra layer of Pt-like atoms is fixed underneath to serve as a frame. In the simulation, the nano-groove has a fixed depth (H) of $35a$ and width (W) of $20a$ but for its hydrophilic pinning site, different sizes (A_i) are introduced ($A_i = 4a \times 4a$, $8a \times 8a$, and $12a \times 12a$). In this work, all the atomic interactions are modeled by the Lennard-Jones (LJ) potential:

$$\varphi(r) = 4\varepsilon\left[\left(\frac{\sigma}{r}\right)^{12} - \left(\frac{\sigma}{r}\right)^{6}\right] \tag{1}$$

where r is the intermolecular separation, ε and σ are the energy and length characteristic parameters, respectively. For the interaction between fluid atoms, $\varepsilon_{ff} = 0.0104$ eV and $\sigma_{ff} = 3.40$

Å. For the interaction between solid atoms, ε_{ss} = 0.521875 eV and σ_{ss} = 2.475 Å. Between solid and fluid atoms, $\varepsilon_{fs} = \beta\varepsilon_{ff}$ and $\sigma_{fs} = 0.91\sigma_{ff}$, where β is fluid-solid bonding strength parameter indicating the surface free energy, or equivalently the surface wettability. A larger value of β suggests higher surface free energy and stronger surface wettability. According to our previous work [35], β = 0.1 is chosen to describe the interaction between atoms of superhydrophobic nanostructured surface and fluid atoms. For the interaction between atoms of local pinning site and fluid atoms, β is chosen to be 0.4 and 1.0, representing hydrophilic and superhydrophilic sites, respectively. For the convenience of later expression, the amphiphilic nanostructured surfaces are labeled as β = (0.1, 0.4) and β = (0.1, 1.0) and the surface wettability of the pinning site is noted by β_i. For all interactions, the potential function is truncated at the cut-off distance $r_c = 3.5\sigma_{ff}$, beyond which atom interactions are ignored.

All the simulations are performed with a time step of 5 fs. In the equilibrium stage, the saturated vapor molecules at T = 115 K are uniformly arranged in the simulation system and the initial 2.5 ns guarantees the system to reach a thermal equilibrium state using a Berendsen thermostat. Afterwards, the surface temperature is suddenly decreased to 84 K to initiate the occurrence of condensation. Simultaneously, a vapor supply region with a thickness of l_z /14 is arranged at the uppermost end, where the temperature and density are maintained at a saturation state. For the fluid except for those in the vapor supply region, the added thermostat is removed and only NVE ensemble is employed.

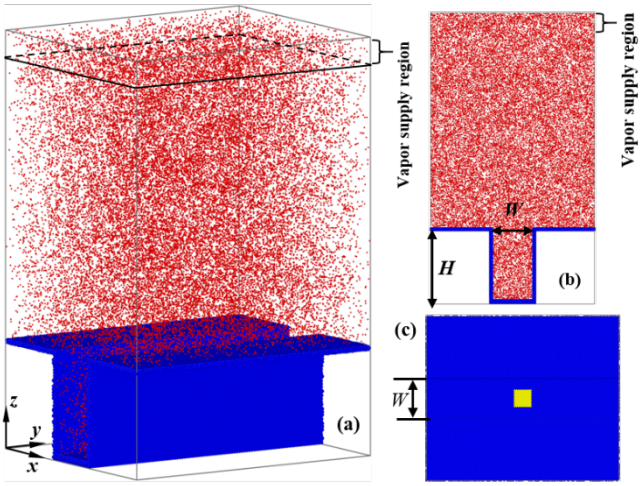

Fig. 1. (a) Schematic of the computational model. Superhydrophobic solid atoms are in blue, hydrophilic solid atoms are in yellow, and fluid molecules are in red. (b) Front view of the simulation system. (c) Top view of the nanostructured surface. H and W represent the depth and width of nano-groove.

3. Results and discussion

3.1 Growth and Self-jumping

To clearly characterize the growth and self-jumping dynamics of single condensed droplet on the nanostructured surface, the nanostructured surface with $\beta = (0.1, 0.4)$ and $A_i = 4a \times 4a$ is chosen here and finally a condensed droplet with radius of 7.5 nm is observed self-jumping from the nanostructured surface. This successfully proves, using MD method, that droplet self-jumping driven by the Laplace pressure difference is also efficient for nano-sized droplet. The snapshots of fluid condensation dynamics are shown in Figure 2a and correspondingly the trajectory of the droplet centroid in the z direction (z_c) is collected (see Figure 2b). On the basis of observations, we generally divide the condensation process before the droplet self-jumping from the nanostructured surface into two stages: incubation and burst stages.

(1) Incubation stage

According to the classical nucleation theory (CNT), surface condensation is a nonspontaneous process and only when the Gibbs free energy barrier is overcome could a nucleus survive and

develop into a droplet. The lower the free energy barrier, the more easily the surface condensation happens. Based on our previous study [35], larger β can diminish the Gibbs free energy barrier and promote the onset of surface condensation. Thus, after the surface temperature drops from 115 to 84 K, a droplet nucleates from the hydrophilic pinning site and then smoothly grows. Due to the confinement from the superhydrophobic groove walls in the *x*-*z* plane, the growth of droplet in this plane is squeezed and naturally deformed to a pancake shape instead of a circular shape (see t = 35 ns in Figure 2a). Comparatively, the droplet freely grows in the *y*-*z* plane parallel to the nano-groove and its shape remains nearly circular (see t = 35 ns in Figure 2a). During this process, the whole droplet is embedded in the groove and the radii of curvature for the bottom interface ($R_b(t)$) and top interface ($R_t(t)$) of the droplet are nearly same, as illustrated in Figure 2c. The top interface of the condensed droplet continuously moves upward with a constant contact angle ($\theta_t(t)$) and $R_t(t)$ due to the occurrence of condensation, see in Figure 2d and 2e. Gradually, the upper front of the growing droplet emerges from the groove and the emerging part frees from the constraint of the groove (see t = 107.5 ns in Figure 2a). When the triple-phase contact line of the top interface reaches the groove edges, the baseline for $\theta_t(t)$ changes from the vertical plane of the groove wall to the horizontal plane of the groove top (see Figure 2c), which leads to a significant drop in $\theta_t(t)$ in Figure 2e. Subsequently, the emerging part of the condensed droplet can also freely grow in the *x*-*z* plane. In this stage, z_c smoothly increases as the droplet grows (see Figure 2b). The measured widest length of the droplet (L_{max}) in the *y*-*z* plane also steadily increases (see Figure 3).

(2) Burst stage

As seen in Figure 2a, after the triple-phase contact line of the top interface reaches the groove edges, the droplet top grows with pinned contact line at the sharp groove edges during the following condensation process. Gradually, we observed that L_{max} starts decreasing due to the

shrinkage of the droplet in the *y*-*z* plane (see Figure 3). The reason of this is that the droplet top can not only freely grow and expand in the *y*-*z* plane but also in the *x*-*z* plane, which makes it recover to a spherical shape due to surface tension. Since then, the growth of the droplet moves to the burst stage and $\theta_t(t)$ and $R_t(t)$ start increasing obviously (see Figure 2d and 2e). In contrast, $R_b(t)$ remains small, and its change is not significant due to the confinement of the groove wall. Thus, as the droplet grows further, a Laplace pressure difference ($\Delta P = \sigma(1/R_b - 1/R_t)$, where σ is the liquid-vapor surface tension of fluid) is built up in the deformed droplet due to the curvature difference. Consequently, an upward force is generated and gradually increases by this Laplace pressure difference. Due to the existence of the local hydrophilic site, there is a strong pinning force preventing the detachment of the droplet from the valley of the groove and the droplet bottom is gradually stretched in the *z* direction. When the droplet top grows to a certain size, the upward force can overcome the significant pinning force and the deformed droplet can detach from the valley of the groove. After detaching from the valley of the groove, the increase rate in the number of condensed molecules (N) of the droplet dramatically decreases, as shown in Figure 4. This is because phase change is a nonspontaneous process, and the cooling effect mainly results from the local hydrophilic site. Once the droplet detaches from the local hydrophilic site, vapor molecules is difficult to condense to liquid molecules due to the high Gibbs free energy barrier for condensation on a superhydrophobic surface. Thus, we can conclude that the droplet growth mainly occurs before the droplet detaches from the local hydrophilic site and the final size of the self-jumping droplet is affected by the feature of the local hydrophilic site.

Relief from the pinning site, the droplet top expands more quickly and the whole droplet fast moves upward due to the significant Laplace pressure difference and subsequently self-jumps from the nanostructured surface (see Figure 2a). Correspondingly, the increases in z_c and R_t become more significant, especially after detaching from the groove valley (see Figure 2b and

2d). From the energy point of view, due to the confinement of the groove, the condensed droplet is deformed, and its surface area is larger than the spherical droplet having the same volume, which leads to the existence of excess surface energy stored in the droplet. After the droplet detaches from the local pinning site, a big part of the excess surface energy converts into kinetic energy, which makes the droplet achieve self-jumping.

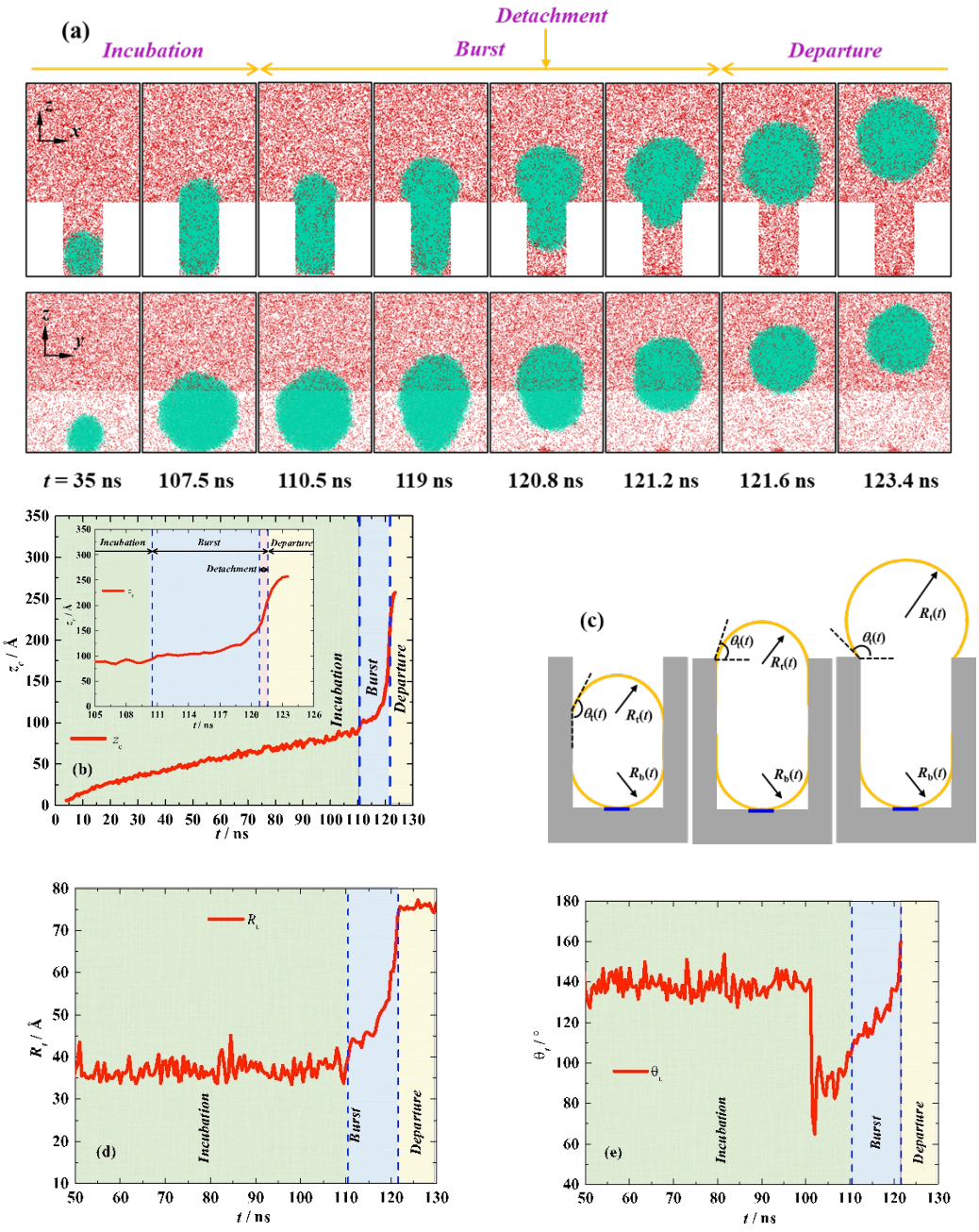

Figure 2. (a) Snapshots of the growth and self-jumping of single condensed droplet from the nanostructured surface with $\beta = (0.1, 0.4)$ and $A_i = 4a \times 4a$. Here only fluid atoms are shown, and the focused condensed droplet is marked in green, and the rest fluid atoms are in red. (b) Trajectory of the droplet centroid in the z direction (z_c).

(c) Schematic of the droplet growth and burst process. (d) Radius of the curvature for the top interface (R_t) of the condensed droplet. (e) Contact angle for the top interface of the condensed droplet (θ).

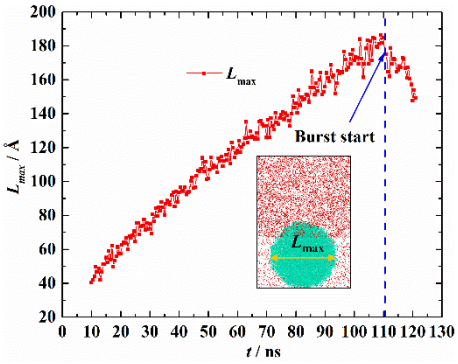

Figure 3. The widest length of the droplet (L_{max}) in the y-z plane parallel to the nano-groove.

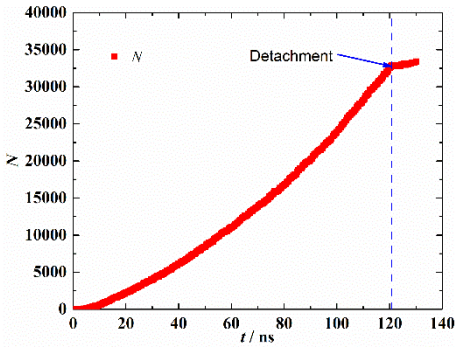

Figure 4. Number of condensed molecules (N) of the focused droplet.

3.2 Jumping velocity

To identify the self-jumping velocity, the velocity of the condensed droplet centroid in the z-direction (v_z) is collected and shown in Figure 5a. It can be seen that v_z essentially fluctuates around 0.005 Å·ps^{-1} before the droplet detaches from the groove valley. The fluctuation and much small nonzero v_z mainly results from the thermal motion of the droplet molecules and the occurrence of condensation [14]. Here, the droplet can be seen static before the droplet detachment from the groove valley occurring. This also shows that due to the pinning effect from the local hydrophilic site, the upward flow from the droplet bottom due to the Laplace pressure difference is accommodated by the static droplet top. The droplet top behaves like an inactive momentum sink and the excessive surface energy makes no direct contribution to

upward kinetic energy. As the droplet top continuously grows larger and establishes a sufficient favorable Laplace pressure difference to overcome the pinning force, the deformed droplet detaches from the groove valley with $v_d = 0.0381$ Å·ps^{-1} (see Figure 5a). Following the droplet detachment from the groove valley, v_z continuously increases significantly as the large excessive surface energy partly converts to kinetic energy and the upward momentum appears after lacking impedance of the pinning force. The stretched droplet bottom quickly adjusts to circular shape, meanwhile the deformed droplet quickly moves upward and tries recovering to a spherical shape. Before the triple-phase contact line of the bottom interface arrives at the groove edges, the droplet bottom moves upward with nearly constant shape and at the same time the droplet top still expands continuously, which leads to the increase in Laplace pressure difference. As a result, v_z significantly increases (see Figure 5a and 5b). As seen in Figure 5b and 5c, after the triple-phase contact line of the bottom interface arrives at the groove edges, the contact line of the bottom interface is pinned at the groove edges and the droplet bottom slowly moves upward, thus $R_b(t)$ increases and the curvature difference between the droplet bottom and top significantly decreases. In terms of energy conservation, during the pinning time at the groove edges, the deformation of the droplet is much small, and the stored excessive surface energy is small, so part of the kinetic energy turns to viscous dissipation, which is significant in nanoscale. Therefore, it is observed that v_z starts decreasing before the droplet completely departs from the nanostructured surface. Finally, the condensed droplet departs the nanostructured surface with $v_z = 0.0643$ Å·ps^{-1}, which is regards as the jumping velocity (v_j) in our work. Note that the droplet-jumping velocity is defined as the instantaneous velocity when the droplet completely detaches from the nanostructured surface here, in other words, there is no contact between the droplet atoms and surface atoms. Therefore, the maximum velocity is not the jumping velocity in our work as there are still point contacts between the condensed droplet and the groove edges in the view from the *x*-*z* plane. After self-jumping from the

nanostructured surface, the droplet has a spherical shape and there is no excessive surface energy stored in the droplet. Due to the viscous dissipation, v_z decreases gradually.

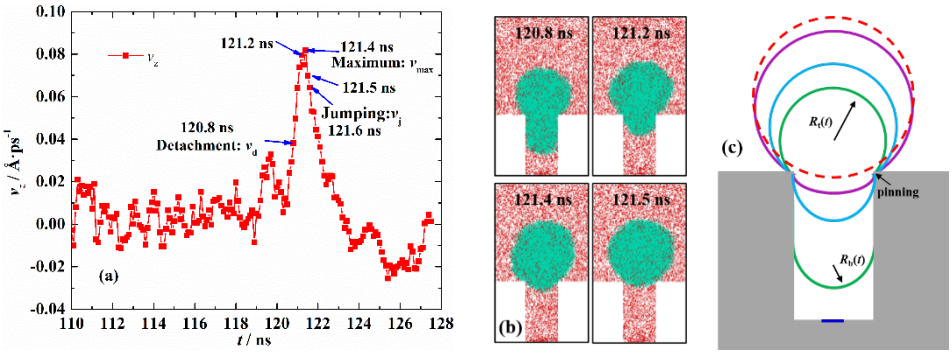

Figure 5. (a) Temporal evolution of velocity of the condensed droplet centroid in the z direction (v_z). (b) Snapshots of dynamical process about droplet moving in the groove after detaching from the groove valley. (c) Schematic showing droplet pinning phenomenon after detaching from the groove valley.

3.3 Local pinning site

According to the abovementioned results, the local hydrophilic pinning site plays an important role in the growth and self-jumping of the droplet. Therefore, the effects of the surface wettability and size of the local pinning site on the whole condensation process is preliminary discussed here.

First, with a fixed pinning size of $A_i = 12a \times 12a$, hydrophilic ($\beta_i = 0.4$) and superhydrophilic ($\beta_i = 1.0$) pinning sites are introduced. The condensation process is compared in Figure 6. Note that the time (t), the number of condensed molecules of the droplet (N) and the radius of the droplet top (R_t) in the x-z plane are also listed for different snapshots. The start of the burst stage, detachment point, and self-jumping point are specially marked with subscripts b, d and j, respectively. Generally, droplets evolve from pinning sites due to their high surface free energy. As the droplet top emerges from the groove, the droplet top starts freely expanding, but the droplet bottom is confined in the groove and gradually stretched. Finally, the droplets detach from the groove valley due to the large Laplace pressure difference in the droplets.

Different from the droplet originating from the pinning site with $\beta_i = 0.4$, which departs the nanostructured surface by self-jumping, the droplet evolving from the pinning site with $\beta_i = 1.0$ does not depart from the nanostructured surface after detaching from the groove valley and stays on the groove top surface. According to our previous study [35], increasing β can promote the occurrence of condensation as it lowers the Gibbs free energy barrier. Thus, the droplet growth for the case with $\beta_i = 1.0$ is faster than that for the case with $\beta_i = 0.4$, and the burst and detachment of the droplet for $\beta_i = 1.0$ case start earlier than those for $\beta_i = 0.4$ case (see Figure 6). But simultaneously the pinning force from the pinning site also increases with the increase in β_i, which means that the droplet top needs to grow larger to have a higher Laplace pressure difference to make itself detach from the groove valley and meanwhile the droplet bottom is stretched more significantly. This is why N_d and R_{td} for $\beta_i = 1.0$ case are observed to be much larger than those for $\beta_i = 0.4$ ($N_d = 37812$ and $R_{td} = 73.7$ Å for $\beta_i = 0.4$ case; $N_d = 75559$ and $R_{td} = 98.6$ Å for $\beta_i = 1.0$ case). According to abovementioned results, the droplet growth nearly stops after detaching from the groove valley, which also proves in these cases. N is nearly constant after droplet detaching from the groove valley and the little fluctuation is due to the thermal motion of fluid molecules. Thus, the final detached droplet on the surface with $\beta_i = 1.0$ is larger than that on the surface with $\beta_i = 0.5$ due to lower Gibbs free energy barrier for the former situation. Additionally, it can also be found that for larger β_i, the droplet bottom is stretched more dramatically before the droplet detaches from the groove valley; it takes significantly longer time to detach from the groove valley after the droplet starts bursting even though the droplet top grows faster for larger β_i. It lasts 17.0 ns from 82.5 to 99.5 ns for $\beta_i = 0.4$ case and 48.7 ns from 38.5 to 87.2 ns for $\beta_i = 0.1$ case. Due to the pinning effect, part of the droplet keeps pinned on the local hydrophilic site thus N drops after the droplet detachment occurs. For larger β_i, the pinning effect is stronger, and the droplet can even be pinched off as

the droplet detachment occurs, then the obvious remainder of the droplet will contract and continue growing (see Figure 6b) from the pinning site. Because of the pinch-off and dramatic stretch of the droplet bottom, the detached droplet has small part squeezed in the groove for larger β_i case, which leads to less excessive free surface energy. Therefore, there is no sufficient kinetic energy converted for the droplet on the surface with larger β_i to support it self-jumping from the surface. Base on those findings, we can conclude that the droplet self-jumping relies on the confined portion of the detached droplet and its decrease can reduce the excessive surface energy stored in the droplet and even make droplet self-jumping from the structured surface fail.

For the effect of the size of local pinning site, with a fixed pinning β_i of 1.0, condensation on the nanostructured surface with pinning sites of $A_i = 4a \times 4a$ and $A_i = 12a \times 12a$ are compared in Figure 7. Comparing t_b, t_d, N_b and N_d, it can be seen that for pinning sites with β_i =1.0, the increasing pinning size can also promote the droplet growth, but this results from increasing the effective heat transfer area where condensation can occur instead of lowering Gibbs free energy barrier. Similar to increasing β_i, the total pinning force gets larger as the pinning size increases. Thus, as the pinning size increases, the droplet top needs to grow larger to make the droplet detach from the groove valley; the droplet bottom is stretched more significantly; the confined portion of the detached droplet decreases significantly, which also leads to the self-jumping fail.

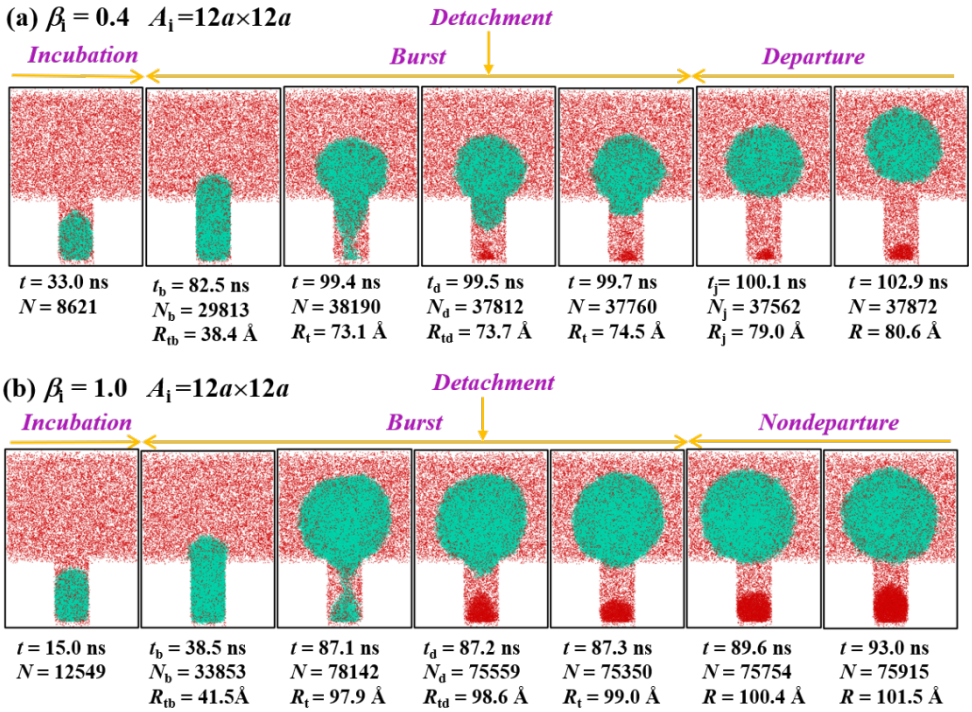

Figure 6 Condensation dynamics on nanostructured surface with local pinning site of (a) $\beta_i = 0.4$ and (b) $\beta_i = 1.0$. The size of the pinning sites (A_i) is both $12a \times 12a$. t, N and R_t are time, number of condensed molecules for the droplet and the radius of the droplet top in the x-z plane, respectively. Subscripts b, d, and j represent the start of the burst stage, detachment point and self-jumping point, respectively.

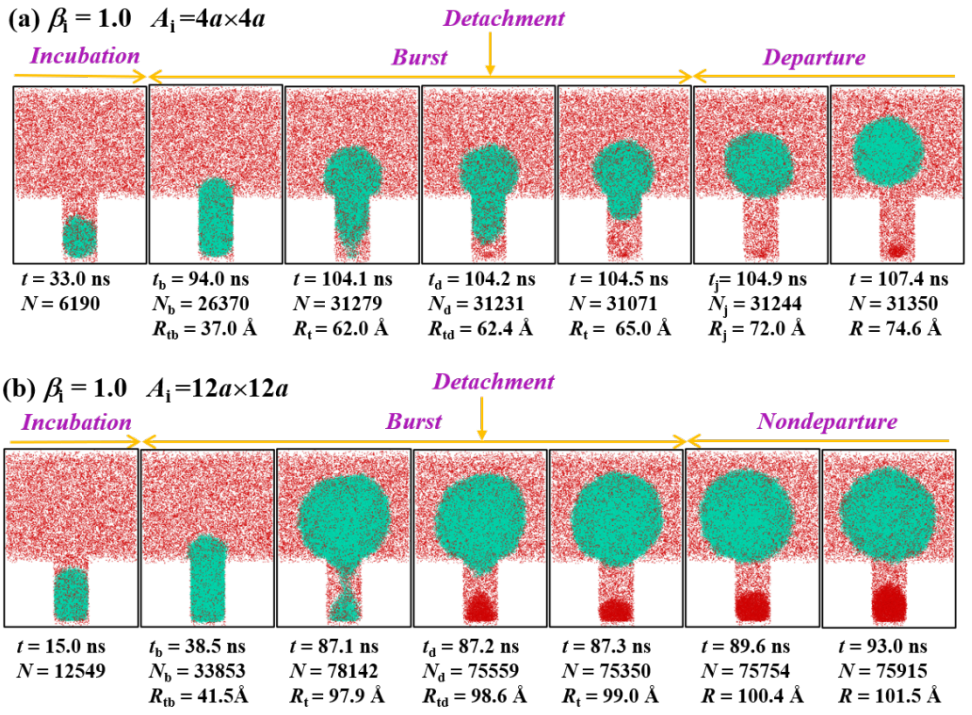

Figure 7 Condensation dynamics on nanostructured surface with local pinning site of (a) $A_i = 4a \times 4a$ and (b) $A_i = 12a \times 12a$, where is the A_i pinning size. The surface wettability of the pinning sites (β_i) is both 1.0. t, N and R_t are time, number of condensed molecules for the droplet and the radius of the droplet top in the x-z plane, respectively. Subscripts b, d, and j represent the start of the burst stage, detachment point and self-jumping point, respectively.

4. Conclusions

In this work, the growth and self-jumping dynamics of single condensed droplet on superhydrophobic nanostructured surface with a local hydrophilic pinning site have been investigated using MD simulations. Our work proves that self-jumping of condensed droplet driven by the Laplace-pressure is effective for nano-size droplet, which has not been previously observed by experiment. In our simulation, a single droplet first evolves from the hydrophilic pinning site and grows in the nanogroove. As its top emerges from the nanogroove, the droplet top gradually grows with pinned contact line at the groove edges and freely expands both laterally and axially down the groove length, but its bottom is still confined in the nanogroove. This deformation leads to a curvature difference between the droplet top and bottom and a Laplace pressure difference is built up in the droplet. When the pressure difference reaches to a certain value, the upward force generated by the pressure difference can overcome the pinning force from the hydrophilic pinning site, which leads to the droplet detaching from the groove valley and finally self-jumping from the nanostructured surface. In this process, droplet growth mainly occurs in the time before the droplet detaching from the groove valley. Additionally, the effects of the surface wettability and size of the pinning site are also preliminarily discussed. Our results show that the hydrophilic pinning site with larger β_i and size can promote the droplet growth but also make the self-jumping harder due to the increase in the total pinning force. The self-jumping of the condensed droplets lies on the confined portion of the detached droplets from the groove valley and its decrease will reduce the excessive surface energy stored

in the droplet, which leads to less kinetic energy converted and it cannot support the droplet self-jumping from the nanostructured surface.

CRediT authorship contribution statement

J.H. Pu: Investigation, Writing - original draft. **S.K. Wang**: Validation, Writing, review & editing. **J Sun**: Supervision, Project administration, Writing - review & editing. **W. Wang**: Validation, Writing - review & editing. **H.S Wang**: Supervision, Project administration, Writing - review & editing.

Declaration of Competing

The authors declare no competing financial interest.

Acknowledgements

This work was supported by the Joint PhD Studentship of China Scholarship Council (CSC) and Queen Mary University of London, National Natural Science Foundation of China (51776196), the Natural Science Foundation of Shaanxi Province (2020JM-048), the Shaanxi Creative Talents Promotion Plan-Technological Innovation Team (2019TD-039), the Fundamental Research Funds for the Central Universities. We are grateful to the UK Materials and Molecular Modelling Hub for computational resources, which is partially funded by EPSRC (EP/P020194/1).

References

[1] Cho, H. J.; Preston, D. J.; Zhu, Y.; Wang, E. N., Nanoengineered materials for liquid–vapour phase-change heat transfer. Nature Reviews Materials 2016, 2 (2), 1-17.

[2] Miljkovic, N.; Wang, E. N., Condensation heat transfer on superhydrophobic surfaces. MRS Bulletin 2013, 38 (5), 397-406.

[3] Rose, J. W., Dropwise condensation theory and experiment: A review. Proceedings of the Institution of Mechanical Engineers, Part A: Journal of Power and Energy 2005, 216 (2), 115-128.

[4] Boreyko, J. B.; Chen, C. H., Restoring superhydrophobicity of lotus leaves with vibration-induced dewetting. Physical review letters 2009, 103 (17), 174502.

[5] Cheng, Z.; Lai, H.; Zhang, N.; Sun, K.; Jiang, L., Magnetically induced reversible transition between Cassie and Wenzel states of superparamagnetic microdroplets on highly hydrophobic silicon surface. The Journal of Physical Chemistry C 2012, 116 (35), 18796-18802.

[6] Wang, Q.; Yao, X.; Liu, H.; Quere, D.; Jiang, L., Self-removal of condensed water on the legs of water striders. Proceedings of the National Academy of Sciences 2015, 112 (30), 9247-52.

[7] Singh, N. S.; Zhang, J.; Stafford, J.; Anthony, C.; Gao, N., Implementing superhydrophobic surfaces within various condensation environments: a review. Advanced Materials Interfaces 2021, 8(2), 2001442.

[8] Anand, S.; Paxson, A. T.; Dhiman, R.; Smith, J. D.; Varanasi, K. K., Enhanced condensation on lubricant-impregnated nanotextured surfaces. ACS nano 2012, 6(11), 10122-10129.

[9] Smith, J. D.; Dhiman, R.; Anand, S.; Reza-Garduno, E.; Cohen, R. E.; McKinley, G. H.; Varanasi, K. K., Droplet mobility on lubricant-impregnated surfaces. Soft Matter 2013, 9(6), 1772-1780.

[10] Guo, L.; Tang, G. H.; Kumar, S., Dynamic wettability on the lubricant-impregnated surface: from nucleation to growth and coalescence. ACS Applied Materials & Interfaces 2020, 12 (23), 26555-26565.

[11] Boreyko, J. B.; Chen, C. H., Self-propelled dropwise condensate on superhydrophobic surfaces. Physical review letters 2009, 103 (18), 184501.

[12] Miljkovic, N.; Enright, R.; Nam, Y.; Lopez, K.; Dou, N.; Sack, J.; Wang, E. N., Jumping-droplet-enhanced condensation on scalable superhydrophobic nanostructured surfaces. Nano Lett 2013, 13 (1), 179-87.

[13] Lv, C.; Hao, P.; Yao, Z.; Niu, F., Departure of condensation droplets on superhydrophobic surfaces. Langmuir 2015, 31 (8), 2414-20.

[14] Liang, Z.; Keblinski, P., Coalescence-induced jumping of nanoscale droplets on super-hydrophobic surfaces. Applied Physics Letters 2015, 107 (14), 143105.

[15] Sheng, Q.; Sun, J.; Wang, W.; Wang, H. S.; Bailey, C. G., How solid surface free energy determines coalescence-induced nanodroplet jumping: A molecular dynamics investigation. Journal of Applied Physics 2017, 122 (24), 245301.

[16] Gao, S.; Liao, Q.; Liu, W.; Liu, Z., Coalescence-induced jumping of nanodroplets on textured surfaces. The journal of physical chemistry letters 2018, 9(1), 13-18.

[17] Yan, X.; Zhang, L.; Sett, S.; Feng, L.; Zhao, C.; Huang, Z.; Vahabi, H.; Kota, A. K.; Chen, F.; Miljkovic, N., Droplet jumping: effects of droplet size, surface structure, pinning, and liquid properties. ACS Nano 2019, 13 (2), 1309-1323.

[18] Mukherjee, R.; Berrier, A. S.; Murphy, K. R.; Vieitez, J. R.; Boreyko, J. B., How surface orientation affects jumping-droplet condensation. Joule 2019, 3 (5), 1360-1376.

[19] Perumanath, S.; Borg, M. K.; Sprittles, J. E.; Enright, R., Molecular physics of jumping nanodroplets. Nanoscale 2020, 12 (40), 20631-20637.

[20] Shi, Y.; Tang, G. H.; Shen, L. Y., Study of coalescence-induced droplet jumping during phase-change process in the presence of noncondensable gas. International Journal of Heat and Mass Transfer 2020, 152, 119506.

[21] Enright, R.; Miljkovic, N.; Sprittles, J.; Nolan, K.; Mitchell, R.; Wang, E. N., How coalescing droplets jump. ACS Nano 2014, 8(10), 10352-10362.

[22] Liu, F.; Ghigliotti, G.; Feng, J. J.; Chen, C.-H., Numerical simulations of self-propelled jumping upon drop coalescence on non-wetting surfaces. Journal of Fluid Mechanics 2014, 752, 39-65.

[23] Lv, C.; Hao, P.; Zhang, X.; He, F., Dewetting transitions of dropwise condensation on nanotexture-enhanced superhydrophobic surfaces. ACS Nano 2015, 9(12), 12311-12319.

[24] Aili, A.; Li, H.; Alhosani, M. H.; Zhang, T., Unidirectional fast growth and forced jumping of stretched droplets on nanostructured microporous surfaces. ACS applied materials & interfaces 2016, 8 (33), 21776-86.

[25] Sharma, C. S.; Combe, J.; Giger, M.; Emmerich, T.; Poulikakos, D., Growth rates and spontaneous navigation of condensate droplets through randomly structured textures. ACS Nano 2017, 11 (2), 1673-1682.

[26] Peng, Q.; Yan, X.; Li, J.; Li, L.; Cha, H.; Ding, Y.; Dang, C.; Jia, L.; Miljkovic, N., Breaking droplet jumping energy conversion limits with superhydrophobic microgrooves. Langmuir 2020, 36 (32), 9510-9522.

[27] Winter, R. L.; McCarthy, M., Dewetting from amphiphilic minichannel surfaces during condensation. ACS applied materials & interfaces 2020, 12 (6), 7815-7825.

[28] Yan, X.; Qin, Y.; Chen, F.; Zhao, G.; Sett, S.; Hoque, M. J.; Rabbi, K. F.; Zhang, X.; Wang, Z.; Li, L.; Chen, F.; Feng, J.; Miljkovic, N., Laplace pressure driven single-droplet jumping on structured surfaces. ACS Nano 2020, 14 (10), 12796-12809.

[29] Niu, D.; Tang, G. H., The effect of surface wettability on water vapor condensation in nanoscale. Scientific reports 2016, 6, 19192.

[30] Sun, J.; Wang, H. S., On the early and developed stages of surface condensation: competition mechanism between interfacial and condensate bulk thermal resistances. Scientific reports 2016, 6, 35003.

[31] Niu, D.; Tang, G., Molecular dynamics simulation of droplet nucleation and growth on a rough surface: revealing the microscopic mechanism of the flooding mode. RSC Advances 2018, 8 (43), 24517-24524.

[32] Pu, J. H.; Sheng, Q.; Sun, J.; Wang, W.; Wang, H. S., Dependence of nano-confined surface condensation on tangentially external force field. Journal of Molecular Liquids 2019, 283, 440-450.

[33] Tang, G.; Niu, D.; Guo, L.; Xu, J., Failure and recovery of droplet nucleation and growth on damaged nanostructures: A Molecular Dynamics study. Langmuir 2020, 36 (45), 13716-13724.

[34] Plimpton, S., Fast parallel algorithms for short-range molecular dynamics. Journal of computational physics 1995, 117(1), 1-19.

[35] Pu, J. H.; Sun, J.; Sheng, Q.; Wang, W.; Wang, H. S., Dependences of formation and transition of the surface condensation mode on wettability and temperature difference. Langmuir 2020, 36 (1), 456-464.